SIAM J. Applied Dynamical Systems
Vol. 5, No. 1, pp. 66–83

Block-Diagonalization of the Symmetric First-Order Coupled-Mode System*

Marina Chugunova† and Dmitry Pelinovsky†

Abstract. We consider the Hamiltonian first-order coupled-mode system that occurs in nonlinear optics, photonics, and atomic physics. Spectral stability of gap solitons is determined by eigenvalues of the linearized coupled-mode system, which is equivalent to a four-by-four Dirac system with sign-indefinite metric. In the special class of symmetric nonlinear potentials, we construct a block-diagonal representation of the linearized equations, when the spectral problem reduces to two coupled two-by-two Dirac systems. The block-diagonalization is used in fast numerical computations of eigenvalues with the Chebyshev interpolation algorithm.

Key words. Hamiltonian first-order coupled-mode systems, gap solitons, spectral stability, invariant subspaces, eigenvalues

AMS subject classifications. 34L16, 37K45, 34L40, 35Q51

DOI. 10.1137/050629781

1. Introduction.

Various applications in nonlinear optics [1], photonics band-gap engineering [2], and atomic physics [3] call for systematic studies of the *coupled-mode system*, which is expressed by two first-order semilinear PDEs in one space and one time dimensions. In nonlinear optics, the coupled-mode system describes counter-propagating light waves, which interact with a linear grating in an optical waveguide [4]. In photonics, the coupled-mode system is derived for coupled resonant waves in stop bands of a low-contrast three-dimensional photonic crystal [5]. In atomic physics, the coupled-mode system describes matter-wave Bose–Einstein condensates trapped in an optical lattice [6]. Existence, stability, and nonlinear dynamics of *gap solitons*, which are localized solutions of the coupled-mode system, are fundamental problems of interest in the aforementioned physical disciplines.

In the context of spectral stability of gap solitons, it has been discovered that the linearized coupled-mode system is equivalent to a four-by-four Dirac system with sign-indefinite metric, where numerical computations of eigenvalues represent a difficult numerical task. The pioneer work in [7, 8] showed that spurious unstable eigenvalues originate from the continuous spectrum in the Fourier basis decomposition and the Galerkin approximation. A delicate but time-consuming implementation of the continuous Newton method was developed to differentiate true unstable eigenvalues from the spurious ones [8]. Similar problems were discovered in the variational method [9, 10] and in the numerical finite-difference method [11, 12].

While some conclusions on instability bifurcations of gap solitons in the coupled-mode equations can be drawn on the basis of perturbation theory [7] and Evans function methods

*Received by the editors April 21, 2005; accepted for publication (in revised form) by J. Meiss August 26, 2005; published electronically January 27, 2006. This work was completed with the support of the SharcNet Graduate Scholarship.
http://www.siam.org/journals/siads/5-1/62978.htmll
†Department of Mathematics, McMaster University, Hamilton, Ontario, L8S 4K1, Canada (chugunom@math.mcmaster.ca, dmpeli@math.mcmaster.ca).

[13, 14], the numerical approximation of eigenvalues was an open problem until recently. New progress was made with the use of exterior algebra in the numerical computations of the Evans function [15], when the results of [7] on instability bifurcations of gap solitons were recovered. A similar shooting method was also applied to gap solitons in a more general model of a nonlinear Schrödinger equation with a periodic potential [6].

Our work addresses the problem of numerical approximations of eigenvalues in the linearized coupled-mode system with a different objective. We will show that the linearized system with a symmetric potential function can be block-diagonalized into two coupled two-by-two Dirac systems. The two Dirac systems represent the linearized Hamiltonian of the coupled-mode equations and determine instability bifurcations and unstable eigenvalues of gap solitons.

The main purpose of block-diagonalization is to optimize a numerical algorithm based on Chebyshev interpolation (see a recent application of Chebyshev interpolation to a system of coupled nonlinear Schrödinger equations in [16]). The algorithm computes the entire spectrum of the linearized coupled-mode system. It also allows us to control the spurious eigenvalues at least near the end points of continuous spectrum, where instability bifurcations occur [7, 15]. Due to block-diagonalization, the algorithm requires two times less memory compared to the standard discretization of the full linearized system, and computations of eigenvalues within the same tolerance bound are accelerated approximately twice as much. We report applications of the numerical algorithm to an example of the linearized coupled-mode system with a symmetric quartic potential function.

The paper is organized as follows. Section 2 describes the model and its symmetries. Section 3 gives the construction and properties of gap solitons in the nonlinear coupled-mode system. Section 4 presents block-diagonalization of the linearized coupled-mode system. Section 5 contains numerical computations of the spectrum of the block-diagonalized system. The appendix deals with exact solutions for gap solitons in the coupled-mode system with symmetric homogeneous potential functions.

2. Coupled-mode system.

We consider the *Hamiltonian* first-order coupled-mode system in the form

$$\begin{cases} i(u_t + u_x) + v = \partial_{\bar{u}} W(u, \bar{u}, v, \bar{v}), \\ i(v_t - v_x) + u = \partial_{\bar{v}} W(u, \bar{u}, v, \bar{v}), \end{cases} \tag{2.1}$$

where $(u, v) \in \mathbb{C}^2$, $x \in \mathbb{R}$, $t \geq 0$, and $W(u, \bar{u}, v, \bar{v})$ is real-valued. We assume that the potential function satisfies the following three conditions:

1. W is invariant with respect to the gauge transformation $(u, v) \mapsto e^{i\alpha}(u, v)$ for all $\alpha \in \mathbb{R}$.
2. W is symmetric with respect to the interchange $(u, v) \mapsto (v, u)$.
3. W is analytic in its variables near $u = v = 0$, such that $W = O(4)$.

The first condition is justified by the standard derivation of the coupled-mode system (2.1) with an envelope approximation [5]. The second condition defines a class of symmetric nonlinear potentials. Although it is somewhat restrictive, symmetric nonlinear potentials are commonly met in physical applications of the system (2.1). The third condition is related to the normal form analysis [17], where the nonlinear functions are approximated by Taylor

polynomials. Since the quadratic part of the potential function W is accounted for in the left-hand side of the system (2.1) and the cubic part of W violates the gauge transformation and analyticity assumptions, the Taylor polynomials of W start with quartic terms denoted as $O(4)$.

We find a general representation of the function $W(u,\bar{u},v,\bar{v})$ that satisfies the conditions 1–3 and list all possible (four-parameter) quartic terms of W.

Lemma 2.1. *If $W \in \mathbb{R}$ and condition 1 is satisfied, such that*

$$W(u,\bar{u},v,\bar{v}) = W\left(ue^{i\alpha}, \bar{u}e^{-i\alpha}, ve^{i\alpha}, \bar{v}e^{-i\alpha}\right) \qquad \forall \alpha \in \mathbb{R}, \tag{2.2}$$

then $W = W(|u|^2, |v|^2, \bar{u}v + u\bar{v})$.

Proof. The statement is a special case of Theorem 1.2 on page 450 of [18]. For the readers' convenience, we give a simplified proof based on the symmetry generator for the gauge transformation. By differentiating (2.2) in α and setting $\alpha = 0$, we derive the relation on $W \in \mathbb{R}$:

$$DW \equiv i\left(u\frac{\partial}{\partial u} - \bar{u}\frac{\partial}{\partial \bar{u}} + v\frac{\partial}{\partial v} - \bar{v}\frac{\partial}{\partial \bar{v}}\right) W(u,\bar{u},v,\bar{v}) = 0. \tag{2.3}$$

Consider the set of quadratic variables

$$z_1 = |u|^2, \quad z_2 = |v|^2, \quad z_3 = \bar{u}v + u\bar{v}, \quad z_4 = u^2 + v^2,$$

which is independent for any $u \neq 0$ and $v \neq 0$ in the sense that the Jacobian is nonzero. It is clear that $Dz_{1,2,3} = 0$ and $Dz_4 = 2iz_4$. Therefore, $DW = 2iz_4\partial_{z_4}W = 0$, such that $W = W(z_1, z_2, z_3)$. ■

Lemma 2.2. *If $W \in \mathbb{R}$ and conditions 1–3 are satisfied, then $W = W(|u|^2 + |v|^2, |u|^2|v|^2, u\bar{v} + v\bar{u})$.*

Proof. By Lemma 2.1 and condition 2, we can reorder the arguments of W as $W = W(|u| + |v|, |u||v|, u\bar{v} + v\bar{u})$. By analyticity in condition (3), W may depend only on $|u|^2$ and $|v|^2$ rather than on $|u|$ and $|v|$. ■

Corollary 2.3. *The only quartic potential function $W \in \mathbb{R}$ that satisfies conditions 1–3 is given by*

$$W = \frac{a_1}{2}(|u|^4 + |v|^4) + a_2|u|^2|v|^2 + a_3(|u|^2 + |v|^2)(v\bar{u} + \bar{v}u) + \frac{a_4}{2}(v\bar{u} + \bar{v}u)^2, \tag{2.4}$$

where (a_1, a_2, a_3, a_4) are real-valued parameters. It follows then that

$$\begin{cases} \partial_{\bar{u}}W = a_1|u|^2u + a_2u|v|^2 + a_3\left[(2|u|^2 + |v|^2)v + u^2\bar{v}\right] + a_4\left[v^2\bar{u} + |v|^2u\right], \\ \partial_{\bar{v}}W = a_1|v|^2v + a_2v|u|^2 + a_3\left[(2|v|^2 + |u|^2)u + v^2\bar{u}\right] + a_4\left[u^2\bar{v} + |u|^2v\right]. \end{cases}$$

The potential function (2.4) with $a_1, a_2 \neq 0$, and $a_3 = a_4 = 0$ represents a standard coupled-mode system for a subharmonic resonance, e.g., in the context of optical gratings with constant Kerr nonlinearity [1]. When $a_1 = a_3 = a_4 = 0$, this system is integrable with inverse scattering and is referred to as the massive Thirring model [19]. When $a_1 = a_2 = 0$ and $a_3, a_4 \neq 0$, the coupled-mode system corresponds to an optical grating with varying,

mean-zero Kerr nonlinearity, where a_3 is the Fourier coefficient of the resonant subharmonic and a_4 is the Fourier coefficient of the nonresonant harmonic [5] (see also [4]).

We rewrite the coupled-mode system (2.1) as a Hamiltonian system in complex-valued matrix-vector notation:

$$\frac{d\mathbf{u}}{dt} = J\nabla H(\mathbf{u}), \tag{2.5}$$

where $\mathbf{u} = (u, \bar{u}, v, \bar{v})^T$,

$$J = \begin{bmatrix} 0 & -i & 0 & 0 \\ i & 0 & 0 & 0 \\ 0 & 0 & 0 & -i \\ 0 & 0 & i & 0 \end{bmatrix} = -J^T,$$

and $H(u, \bar{u}, v, \bar{v}) = \int_{\mathbb{R}} h(u, \bar{u}, v, \bar{v})dx$ is the Hamiltonian functional with the density

$$h = W(u, \bar{u}, v, \bar{v}) - (v\bar{u} + u\bar{v}) + \frac{i}{2}(u\bar{u}_x - u_x\bar{u}) - \frac{i}{2}(v\bar{v}_x - v_x\bar{v}).$$

The Hamiltonian $H(u, \bar{u}, v, \bar{v})$ is constant in time $t \geq 0$. Due to the gauge invariance, the coupled-mode system (2.1) has another constant of motion $Q(u, \bar{u}, v, \bar{v})$, where

$$Q = \int_{\mathbb{R}} \left(|u|^2 + |v|^2 \right) dx. \tag{2.6}$$

Conservation of Q can be checked by direct computation:

$$\frac{\partial}{\partial t}(|u|^2 + |v|^2) + \frac{\partial}{\partial x}(|u|^2 - |v|^2) = DW = 0, \tag{2.7}$$

where the operator D is defined in (2.3). Due to the translational invariance, the coupled-mode system (2.1) has yet another constant of motion $P(u, \bar{u}, v, \bar{v})$, where

$$P = \frac{i}{2} \int_{\mathbb{R}} \left(u\bar{u}_x - u_x\bar{u} + v\bar{v}_x - v_x\bar{v} \right) dx. \tag{2.8}$$

In applications, the quantities Q and P are referred to as the power and momentum of the coupled-mode system.

3. Existence of gap solitons. *Stationary* solutions of the coupled-mode system (2.1) take the form

$$\begin{cases} u_{\rm st}(x,t) = u_0(x+s)e^{i\omega t + i\theta}, \\ v_{\rm st}(x,t) = v_0(x+s)e^{i\omega t + i\theta}, \end{cases} \tag{3.1}$$

where $(s, \theta) \in \mathbb{R}^2$ are arbitrary parameters, while the solution $(u_0, v_0) \in \mathbb{C}^2$ on $x \in \mathbb{R}$ and the domain for parameter $\omega \in \mathbb{R}$ are to be found from the nonlinear ODE system

$$\begin{cases} iu_0' = \omega u_0 - v_0 + \partial_{\bar{u}_0} W(u_0, \bar{u}_0, v_0, \bar{v}_0), \\ -iv_0' = \omega v_0 - u_0 + \partial_{\bar{v}_0} W(u_0, \bar{u}_0, v_0, \bar{v}_0). \end{cases} \tag{3.2}$$

Stationary solutions are critical points of the Lyapunov functional

$$\Lambda = H(u,\bar{u},v,\bar{v}) + \omega Q(u,\bar{u},v,\bar{v}), \tag{3.3}$$

such that variations of Λ produce the nonlinear ODE system (3.2).

Lemma 3.1. *Assume that there exists a decaying solution (u_0, v_0) of the system (3.2) on $x \in \mathbb{R}$. If $W \in \mathbb{R}$ and conditions 1–3 are satisfied, then $u_0 = \bar{v}_0$ (modulo to an arbitrary phase).*

Proof. It follows from the balance equation (2.7) for the stationary solutions (3.1) that

$$|u_0|^2 - |v_0|^2 = C_0 = 0 \qquad \forall x \in \mathbb{R},$$

where the constant $C_0 = 0$ is found from decaying conditions at infinity. Let us represent the solutions (u_0, v_0) in the form

$$\begin{cases} u_0(x) = \sqrt{Q(x)} e^{i\Theta(x)+i\Phi(x)}, \\ v_0(x) = \sqrt{Q(x)} e^{-i\Theta(x)+i\Phi(x)}, \end{cases} \tag{3.4}$$

such that

$$\begin{cases} iQ' - 2Q(\Theta' + \Phi') = 2\omega Q - 2Qe^{-2i\Theta} + 2\bar{u}_0 \partial_{\bar{u}_0} W(u_0,\bar{u}_0,v_0,\bar{v}_0), \\ -iQ' - 2Q(\Theta' - \Phi') = 2\omega Q - 2Qe^{2i\Theta} + 2\bar{v}_0 \partial_{\bar{v}_0} W(u_0,\bar{u}_0,v_0,\bar{v}_0). \end{cases} \tag{3.5}$$

Separating the real parts, we obtain

$$\begin{cases} Q(\cos(2\Theta) - \omega - \Theta' - \Phi') = \mathrm{Re}\left[\bar{u}_0 \partial_{\bar{u}_0} W(u_0,\bar{u}_0,v_0,\bar{v}_0)\right], \\ Q(\cos(2\Theta) - \omega - \Theta' + \Phi') = \mathrm{Re}\left[\bar{v}_0 \partial_{\bar{v}_0} W(u_0,\bar{u}_0,v_0,\bar{v}_0)\right]. \end{cases} \tag{3.6}$$

It follows from Lemma 2.2 that

$$\left(u\frac{\partial}{\partial u} + \bar{u}\frac{\partial}{\partial \bar{u}} - v\frac{\partial}{\partial v} - \bar{v}\frac{\partial}{\partial \bar{v}} \right) W(u,\bar{u},v,\bar{v}) \Big|_{|u|^2=|v|^2} = 0. \tag{3.7}$$

As a result, we have $\Phi' \equiv 0$, such that $\Phi(x) = \Phi_0$. ∎

Corollary 3.2. *Let $u_0 = \bar{v}_0$. The ODE system (3.2) reduces to the planar Hamiltonian form*

$$\frac{d}{dx}\begin{pmatrix} p \\ q \end{pmatrix} = \begin{pmatrix} 0 & -1 \\ +1 & 0 \end{pmatrix} \nabla h(p,q), \tag{3.8}$$

where $p = 2\Theta$, $q = Q$, and

$$h = \tilde{W}(p,q) - 2q\cos p + 2\omega q, \qquad \tilde{W}(p,q) = W(u_0,\bar{u}_0,v_0,\bar{v}_0). \tag{3.9}$$

Proof. In variables (Q,Θ) defined by (3.4) with $\Phi(x) = \Phi_0 \equiv 0$, we rewrite the ODE system (3.5) as follows:

$$\begin{cases} Q' = 2Q\sin(2\Theta) + 2\mathrm{Im}\left[\bar{u}_0 \partial_{\bar{u}_0} W(u_0,\bar{u}_0,v_0,\bar{v}_0)\right], \\ Q\Theta' = -\omega Q + Q\cos(2\Theta) - \mathrm{Re}\left[\bar{u}_0 \partial_{\bar{u}_0} W(u_0,\bar{u}_0,v_0,\bar{v}_0)\right]. \end{cases} \tag{3.10}$$

The system (3.10) is equivalent to the Hamiltonian system (3.8)–(3.9) if

$$\left\{ \begin{array}{l} \partial_p \tilde{W}(p,q) = i \left[u_0 \partial_{u_0} - \bar{u}_0 \partial_{\bar{u}_0} \right] W(u_0, \bar{u}_0, v_0, \bar{v}_0), \\ q \partial_q \tilde{W}(p,q) = \left[u_0 \partial_{u_0} + \bar{u}_0 \partial_{\bar{u}_0} \right] W(u_0, \bar{u}_0, v_0, \bar{v}_0). \end{array} \right. \tag{3.11}$$

The latter equation follows from (2.3), (3.4), and (3.7) with the chain rule. ■

Remark 3.3. The family of *stationary* solutions (3.1) can be extended to the family of *traveling* solutions of the coupled-mode system (2.1) by means of the Lorentz transformation [15]. When the boosted variables are applied to the form (3.1),

$$X = \frac{x - ct}{\sqrt{1-c^2}}, \quad T = \frac{t - cx}{\sqrt{1-c^2}}, \quad U = \left(\frac{1-c}{1+c} \right)^{1/4} u, \quad V = \left(\frac{1+c}{1-c} \right)^{1/4} v,$$

where $c \in (-1,1)$, the family of traveling solutions (U_0, V_0) satisfies the constraint $|U_0|^2 = |V_0|^2$ from the balance equation (2.7). However, the representation (3.4) results no longer in the relation $U_0 = \bar{V}_0$, since the relation (3.7) fails for the potential function W in boosted variables $(U, \bar{U}, V, \bar{V})$.

Decaying solutions of the system (3.2) with a homogeneous polynomial function $W(u, \bar{u}, v, \bar{v})$ are analyzed in the appendix. Conditions for their existence are identified for the quartic potential function (2.4). Decaying solutions may exist in the gap of the continuous spectrum of the coupled-mode system (2.1) for $\omega \in (-1, 1)$. We introduce two auxiliary parameters

$$\mu = \frac{1-\omega}{1+\omega}, \qquad \beta = \sqrt{1-\omega^2}, \tag{3.12}$$

such that $0 < \mu < \infty$ and $0 < \beta \leq 1$. When $a_1 = 1$, $a_2 = \rho \in \mathbb{R}$, and $a_3 = a_4 = 0$, we obtain in the appendix the decaying solution $u_0(x)$ in the explicit form

$$u_0 = \sqrt{\frac{2(1-\omega)}{1+\rho}} \frac{1}{(\cosh \beta x + i \sqrt{\mu} \sinh \beta x)}. \tag{3.13}$$

When $\omega \to 1$ (such that $\mu \to 0$ and $\beta \to 0$), the decaying solution (3.13) becomes small in absolute value and approaches the limit of sech-solutions $\mathrm{sech}(\beta x)$. When $\omega \to -1$ (such that $\mu \to \infty$ and $\beta \to 0$), the decaying solution (3.13) remains finite in absolute value and approaches the limit of the algebraically decaying solution:

$$u_0 = \frac{2}{\sqrt{1+\rho}(1+2ix)}.$$

When $a_1 = a_2 = 0, a_3 = 1$, and $a_4 = s \in \mathbb{R}$, the decaying solution $u_0(x)$ exists in two subdomains: $0 < \omega < 1$, $s > -1$ and $-1 < \omega < 0$, $s < 1$. When $0 < \omega < 1$, $s > -1$, the solution takes the form

$$u_0 = \sqrt{\frac{1-\omega}{2}} \frac{(\cosh \beta x - i \sqrt{\mu} \sinh \beta x)}{\sqrt{\Delta_+(x)}}, \tag{3.14}$$

where

$$\Delta_+ = [(s-1)\mu^2 - 2s\mu + (s+1)] \cosh^4(\beta x) + 2[s\mu - (s-1)\mu^2] \cosh^2(\beta x) + (s-1)\mu^2.$$

When $-1 < \omega < 0$, $s < 1$, the solution takes the form

$$u_0 = \sqrt{\frac{1-\omega}{2}} \frac{(\sinh \beta x - i\sqrt{\mu} \cosh \beta x)}{\sqrt{\Delta_-(x)}}, \tag{3.15}$$

where

$$\Delta_- = [(s+1) - 2s\mu - (s-1)\mu^2] \cosh^4(\beta x) + 2[s+1-s\mu] \cosh^2(\beta x) - (s+1).$$

In both limits $\omega \to 1$ and $\omega \to -1$, the decaying solutions (3.14) and (3.15) approach the small-amplitude sech-solution $\text{sech}(\beta x)$. In the limit $\omega \to 0$, the decaying solutions (3.14) and (3.15) degenerate into a nondecaying bounded solution with $|u_0(x)|^2 = \frac{1}{2}$.

4. Block-diagonalization of the linearized system. *Linearization* of the coupled-mode system (2.1) at the stationary solutions (3.1) with $s = \theta = 0$ is defined as follows:

$$\begin{cases} u(x,t) = e^{i\omega t}\left(u_0(x) + U_1(x)e^{\lambda t}\right), \\ \bar{u}(x,t) = e^{-i\omega t}\left(\bar{u}_0(x) + U_2(x)e^{\lambda t}\right), \\ v(x,t) = e^{i\omega t}\left(v_0(x) + U_3(x)e^{\lambda t}\right), \\ \bar{v}(x,t) = e^{-i\omega t}\left(\bar{v}_0(x) + U_4(x)e^{\lambda t}\right), \end{cases} \tag{4.1}$$

where $v_0 = \bar{u}_0$, according to Lemma 3.1. Let $(\mathbf{f}, \mathbf{g})$ be a standard inner product for $\mathbf{f}, \mathbf{g} \in L^2(\mathbb{R}, \mathbb{C}^4)$. Expanding the Lyapunov functional (3.3) into Taylor series near $\mathbf{u}_0 = (u_0, \bar{u}_0, v_0, \bar{v}_0)^T$, we have

$$\Lambda = \Lambda(\mathbf{u_0}) + (\mathbf{U}, \nabla\Lambda|_{\mathbf{u}_0}) + \frac{1}{2}(\mathbf{U}, H_\omega \mathbf{U}) + \cdots, \tag{4.2}$$

where $\mathbf{U} = (U_1, U_2, U_3, U_4)^T$, $\nabla\Lambda|_{\mathbf{u}_0} = 0$, and H_ω is the linearized energy operator in the explicit form

$$H_\omega = D(\partial_x) + V(x), \tag{4.3}$$

where

$$D = \begin{pmatrix} \omega - i\partial_x & 0 & -1 & 0 \\ 0 & \omega + i\partial_x & 0 & -1 \\ -1 & 0 & \omega + i\partial_x & 0 \\ 0 & -1 & 0 & \omega - i\partial_x \end{pmatrix} \tag{4.4}$$

and

$$V = \begin{pmatrix} \partial^2_{\bar{u}_0 u_0} & \partial^2_{\bar{u}_0^2} & \partial^2_{\bar{u}_0 v_0} & \partial^2_{\bar{u}_0 \bar{v}_0} \\ \partial^2_{u_0^2} & \partial^2_{u_0 \bar{u}_0} & \partial^2_{u_0 v_0} & \partial^2_{u_0 \bar{v}_0} \\ \partial^2_{\bar{v}_0 u_0} & \partial^2_{\bar{v}_0 \bar{u}_0} & \partial^2_{\bar{v}_0 v_0} & \partial^2_{\bar{v}_0^2} \\ \partial^2_{v_0 u_0} & \partial^2_{v_0 \bar{u}_0} & \partial^2_{v_0^2} & \partial^2_{v_0 \bar{v}_0} \end{pmatrix} W(u_0, \bar{u}_0, v_0, \bar{v}_0). \tag{4.5}$$

The linearization (4.1) reduces the nonlinear coupled-mode system (2.1) to the linear eigenvalue problem in the form

$$H_\omega \mathbf{U} = i\lambda\sigma\mathbf{U}, \tag{4.6}$$

where σ is a diagonal matrix of $(1,-1,1,-1)$. Due to the gauge and translational symmetries, the energy operator H_ω has a two-dimensional kernel with the eigenvectors:

$$\mathbf{U}_1 = \sigma\mathbf{u}_0(x), \qquad \mathbf{U}_2 = \mathbf{u}_0'(x). \tag{4.7}$$

The eigenvectors $\mathbf{U}_{1,2}$ represent derivatives of the stationary solutions (3.1) with respect to parameters (θ, s).

Due to the Hamiltonian structure, the linearized operator σH_ω has at least a four-dimensional generalized kernel with the eigenvectors (4.7) and two generalized eigenvectors (see [20] for details). The eigenvectors of the linearized operator σH_ω satisfy the σ-orthogonality constraints

$$(\sigma\mathbf{u}_0, \sigma\mathbf{U}) = \int_{\mathbb{R}} (\bar{u}_0 U_1 + u_0 U_2 + \bar{v}_0 U_3 + v_0 U_4)\, dx = 0, \tag{4.8}$$

$$(\mathbf{u}_0', \sigma\mathbf{U}) = \int_{\mathbb{R}} (\bar{u}_0' U_1 - u_0' U_2 + \bar{v}_0' U_3 - v_0' U_4)\, dx = 0. \tag{4.9}$$

The constraints (4.8) and (4.9) represent first variations of the conserved quantities Q and P in (2.6) and (2.8) at the linearization (4.1).

When the constraint $u_0 = \bar{v}_0$ holds, the potential part (4.5) has additional symmetry relations:

$$\partial^2_{u_0\bar{u}_0} W = \partial^2_{v_0\bar{v}_0} W, \quad \partial^2_{\bar{u}_0^2} W = \partial^2_{v_0^2} W, \quad \partial^2_{u_0 v_0} W = \partial^2_{\bar{u}_0\bar{v}_0} W. \tag{4.10}$$

It follows from the explicit form of H_ω and the relations (4.10) that the eigenvalue problem $H_\omega \mathbf{U} = \mu\mathbf{U}$ has two reductions:

$$\text{(i) } U_1 = U_4,\ U_2 = U_3, \qquad \text{(ii) } U_1 = -U_4,\ U_2 = -U_3. \tag{4.11}$$

Our main result on the block-diagonalization of the energy operator H_ω and the linearized operator σH_ω is based on the reductions (4.11).

Theorem 4.1. *Let $W \in \mathbb{R}$ and conditions 1–3 are satisfied. Let (u_0, v_0) be a decaying solution of the system (3.2) on $x \in \mathbb{R}$ with the constraint $v_0 = \bar{u}_0$. There exists an orthogonal similarity transformation S, such that $S^{-1} = S^T$, where*

$$S = \frac{1}{\sqrt{2}} \begin{pmatrix} 1 & 0 & 1 & 0 \\ 0 & 1 & 0 & 1 \\ 0 & 1 & 0 & -1 \\ 1 & 0 & -1 & 0 \end{pmatrix},$$

that simultaneously block-diagonalizes the energy operator H_ω,

$$S^{-1} H_\omega S = \begin{pmatrix} H_+ & 0 \\ 0 & H_- \end{pmatrix} \equiv H, \tag{4.12}$$

and the linearized operator σH_ω

$$S^{-1}\sigma H_\omega S = \sigma \begin{pmatrix} 0 & H_- \\ H_+ & 0 \end{pmatrix} \equiv iL, \tag{4.13}$$

where $H_\pm$ *are two-by-two Dirac operators:*

$$H_\pm = \begin{pmatrix} \omega - i\partial_x & \mp 1 \\ \mp 1 & \omega + i\partial_x \end{pmatrix} + V_\pm(x) \tag{4.14}$$

and

$$V_\pm = \begin{pmatrix} \partial^2_{\bar{u}_0 u_0} \pm \partial^2_{\bar{u}_0 \bar{v}_0} & \partial^2_{\bar{u}_0^2} \pm \partial^2_{\bar{u}_0 v_0} \\ \partial^2_{u_0^2} \pm \partial^2_{u_0 \bar{v}_0} & \partial^2_{\bar{u}_0 u_0} \pm \partial^2_{u_0 v_0} \end{pmatrix} W(u_0, \bar{u}_0, v_0, \bar{v}_0). \tag{4.15}$$

Proof. Applying the similarity transformation to the operator $D(\partial_x)$ in (4.4), we have the first term in Dirac operators $H_\pm$. Applying the same transformation to the potential $V(x)$ in (4.5) and using the relations (4.10), we have the second term in Dirac operators $H_\pm$. The same transformation is applied similarly to the linearized operator σH_ω with the result (4.13). ■

Corollary 4.2. (a) *The coupled eigenvalue problem* (4.6) *is equivalent to the block-diagonalized eigenvalue problems*

$$\sigma_3 H_- \sigma_3 H_+ \mathbf{V}_1 = \gamma \mathbf{V}_1, \qquad \sigma_3 H_+ \sigma_3 H_- \mathbf{V}_2 = \gamma \mathbf{V}_2, \qquad \gamma = -\lambda^2, \tag{4.16}$$

where $\mathbf{V}_{1,2} \in \mathbb{C}^2$ *and* σ_3 *is Pauli's diagonal matrix of* $(1, -1)$.

(b) *Let* $\mathbf{u}_0 = (u_0, \bar{u}_0) \in \mathbb{C}^2$ *and* $(\mathbf{f}, \mathbf{g})$ *be a standard inner product for* $\mathbf{f}, \mathbf{g} \in L^2(\mathbb{R}, \mathbb{C}^2)$. *Dirac operators* $H_\pm$ *have simple kernels with the eigenvectors*

$$H_+ \mathbf{u}_0' = 0, \qquad H_- \sigma_3 \mathbf{u}_0 = 0, \tag{4.17}$$

while the vectors $\mathbf{V}_{1,2}$ *satisfy the constraints*

$$(\sigma_3 \mathbf{u}_0, \sigma_3 \mathbf{V}_1) = 0, \qquad (\mathbf{u}_0', \sigma_3 \mathbf{V}_2) = 0. \tag{4.18}$$

Remark 4.3. Block-diagonalization described in Theorem 4.1 has nothing in common with the explicit diagonalization used in the reduction (9.2) of [14] for the particular potential function (2.4) with $a_1 = a_2 = a_4 = 0$ and $a_3 = 1$. Moreover, the reduction (9.2) of [14] does not work for $\omega \neq 0$, while gap solitons do not exist in this particular model for $\omega = 0$.

We apply Theorem 4.1 to the linearized coupled-mode system with the quartic potential function (2.4). When $a_1 = 1$, $a_2 = \rho$, and $a_3 = a_4 = 0$, the decaying solution $u_0(x)$ is given by (3.13) and the potential matrices $V_\pm(x)$ in the Dirac operators $H_\pm$ in (4.14)–(4.15) are found in the explicit form

$$V_+ = (1+\rho) \begin{pmatrix} 2|u_0|^2 & u_0^2 \\ \bar{u}_0^2 & 2|u_0|^2 \end{pmatrix}, \qquad V_- = \begin{pmatrix} 2|u_0|^2 & (1-\rho)u_0^2 \\ (1-\rho)\bar{u}_0^2 & 2|u_0|^2 \end{pmatrix}. \tag{4.19}$$

When $a_1 = a_2 = 0$, $a_3 = 1$, and $a_4 = s$, the decaying solution $u_0(x)$ is given by either (3.14) or (3.15) and the potential matrices $V_\pm(x)$ take the form

$$V_+ = 3 \begin{pmatrix} u_0^2 + \bar{u}_0^2 & 2|u_0|^2 \\ 2|u_0|^2 & u_0^2 + \bar{u}_0^2 \end{pmatrix} + s \begin{pmatrix} 2|u_0|^2 & u_0^2 + 3\bar{u}_0^2 \\ \bar{u}_0^2 + 3u_0^2 & 2|u_0|^2 \end{pmatrix}, \tag{4.20}$$

$$V_- = \begin{pmatrix} u_0^2 + \bar{u}_0^2 & -2|u_0|^2 \\ -2|u_0|^2 & u_0^2 + \bar{u}_0^2 \end{pmatrix} + s \begin{pmatrix} 0 & -u_0^2 - \bar{u}_0^2 \\ -u_0^2 - \bar{u}_0^2 & 0 \end{pmatrix}. \tag{4.21}$$

Numerical computations of eigenvalues of the Dirac operators $H_\pm$ and the linearized operator L in (4.12) and (4.13) are developed for the explicit examples (4.19) and (4.20)–(4.21).

5. Numerical computations of eigenvalues. Numerical discretization and truncation of the linearized system (4.6) leads to an eigenvalue problem for large matrices [21]. Parallel software libraries were recently developed for computations of large eigenvalue problems [22]. We shall use the Scalapack library and distribute computations of eigenvalues of the system (4.6) for different parameter values between parallel processors of the SHARCnet cluster Idra using Message Passing Interface.[1]

We implement a numerical discretization of the linearized system (4.6) using the Chebyshev interpolation method [23]. Given a function $u(z)$ defined on the discrete grid of Chebyshev points $z_j = \cos(j\pi/N), j = 0, 1 \ldots N$, we obtain a discretization of the first derivative $u'(z)$ as a multiplication of the vector for values of $u(z)$ on the discrete grid by an $(N+1)$-by-$(N+1)$ matrix, which we denote by $D_N^{(1)}$. If the rows and columns of the differentiation matrix $D_N^{(1)}$ are indexed from 0 to N, the entries of $D_N^{(1)}$ are (see [24] for details)

$$(D_N^{(1)})_{00} = \frac{2N^2+1}{6}, \quad (D_N^{(1)})_{NN} = -\frac{2N^2+1}{6},$$
$$(D_N^{(1)})_{jj} = \frac{-z_j}{2(1-z_j^2)}, \quad j = 1, \ldots, N-1,$$

and

$$(D_N^{(1)})_{ij} = \frac{c_i}{c_j} \frac{(-1)^{i+j}}{(z_i - z_j)}, \quad i \neq j, \quad i, j = 0, \ldots, N,$$

where $c_0 = c_N = 2$ and $c_i = 1$, $i = 1, \ldots, N-1$. To transform the Chebyshev grid from the interval $z \in [-1, 1]$ to the infinite domain $x \in \mathbb{R}$ we will use the exponential map $f(z) = L \tanh^{-1} z$, such that $x_j = f(z_j)$, $j = 0, 1, \ldots, N$. This map is efficient in our case because the potential matrices $V_\pm(x)$ decay exponentially as $|x| \to \infty$. The constant L sets the length scale of the map and we pick up the values of L such that the localization of matrix potentials $V_\pm(x)$ has a sufficient resolution on the discrete grid points.

Using the chain rule, we represent differentiation of $u(x)$ on the discrete grid with the matrix multiplication

$$\mathbf{p} = \left[\left(\frac{\partial f^{-1}(x_i)}{\partial x} D_N^{(1)} \right) u(z_j), j = 0, 1, \ldots, N \right] \equiv D_{N+1} \mathbf{u},$$

[1] Cluster Idra is a part of the SHARCnet network of parallel processors distributed between eight universities in southern Ontario, including McMaster University.

Table 1

Maximum real part of eigenvalues $M = \max|\mathrm{Re}(\lambda)|$ versus the number of Chebyshev polynomials N for two computational intervals $|\mathrm{Im}(\lambda)| < 2$ and $|\mathrm{Im}(\lambda)| < 10$.

N	$M_{\lvert\mathrm{Im}\lambda\rvert<2}$	$M_{\lvert\mathrm{Im}\lambda\rvert<10}$
100	0.085	0.75
200	0.0095	0.52
400	0.0053	0.21
800	$7.12 \cdot 10^{-4}$	0.12
1200	$2.34 \cdot 10^{-4}$	0.09
2500	$3.91 \cdot 10^{-5}$	0.06

where $\mathbf{u}$ is the vector for values of $u(x)$ and $\mathbf{p}$ is the vector for values of $u'(x)$ on the discrete grid. The discretization of the Dirac operators $H_\pm$ is defined by

$$H_\pm = \begin{pmatrix} \omega I_{N+1} - iD_{N+1} & \mp I_{N+1} \\ \mp I_{N+1} & \omega I_{N+1} + iD_{N+1} \end{pmatrix} + \mathrm{diag} V_\pm(x_i), \tag{5.1}$$

where I_{N+1} is the identity $(N+1)$-by-$(N+1)$ matrix.

The continuous spectrum for the linearized coupled-mode system (4.6) can be found from the no-potential case $V(x) \equiv 0$. It consists of two pairs of symmetric branches on the imaginary axis $\lambda \in i\mathbb{R}$ for $|\mathrm{Im}(\lambda)| > 1 - \omega$ and $|\mathrm{Im}(\lambda)| > 1 + \omega$ [7, 15]. In the potential case $V(x) \neq 0$, the continuous spectrum does not move, but the discrete spectrum appears. The discrete spectrum is represented by symmetric pairs or quartets of isolated nonzero eigenvalues and a zero eigenvalue of algebraic multiplicity four for the generalized kernel of σH_ω [7, 15]. We note that symmetries of the Chebyshev grid preserve symmetries of the linearized coupled-mode system (4.6).

The main advantage of the Chebyshev grid is the clustering distribution of the grid points that enables us to control spurious complex eigenvalues. If the eigenvector is analytic in a strip near the interpolation interval, the corresponding Chebyshev spectral derivatives converge geometrically, with an asymptotic convergence factor determined by the size of the largest ellipse in the domain of analyticity [23].

Spurious complex eigenvalues arise from the discretization of the continuous spectrum. When the number of Chebyshev polynomials increases, the real parts of spurious eigenvalues get smaller. Convergence of real parts of eigenvalues to zero is better near the end points of the continuous spectrum $\lambda = \pm i(1-\omega)$ and $\lambda = \pm i(1+\omega)$, from which bifurcations of true unstable eigenvalues are expected to occur (due to analytical results in [7, 13] and numerical results in [7, 15]). Table 1 shows the maximum real part $M = \max|\mathrm{Re}(\lambda)|$ versus N in two computational intervals $|\mathrm{Im}(\lambda)| < 2$ and $|\mathrm{Im}(\lambda)| < 10$ for the linear eigenvalue problem (4.6) with no true unstable eigenvalues. When $N = 2500$, the real parts of spurious eigenvalues in the interval $|\mathrm{Im}(\lambda)| < 2$ are of the order of 10^{-5}. Using more polynomials, we can make the real parts of the eigenvalues of continuous spectrum negligibly small, so that edge bifurcations of unstable eigenvalues can be studied numerically within any required accuracy.

We compute eigenvalues of the energy operator H_ω and the linearized operator σH_ω. It is well known [21, 23] that Hermitian matrices have condition number one, while non-Hermitian matrices may have a large condition number. As a result, numerical computations

Table 2

CPU time T for block-diagonal and full matrices versus the number of Chebyshev points N.

N	T_{block}	T_{full}
100	1.656	1.984
200	11.219	12.921
400	130.953	207.134
800	997.843	$1.583 \cdot 10^3$
1200	$3.608 \cdot 10^3$	$6.167 \cdot 10^3$
2500	$7.252 \cdot 10^3$	$12.723 \cdot 10^3$

for eigenvalues and eigenvectors have better accuracy and faster convergence for self-adjoint operators [21, 23]. We will use the block-diagonalizations (4.12) and (4.13) and compute eigenvalues of H_+, H_-, and L. The block-diagonalized matrix can be stored in a special format which requires two times less memory than a full matrix and it accelerates computations of eigenvalues approximately twice as much. Table 2 shows CPU time T for computations of eigenvalues of σH_ω for block-diagonal and full matrices versus the number of Chebyshev points N. When $N = 2500$, T_{full} is almost twice as large as T_{block}.

Figure 1 displays the pattern of eigenvalues and instability bifurcations for the symmetric quartic potential (2.4) with $a_1 = 1$ and $a_2 = a_3 = a_4 = 0$. The decaying solution $u_0(x)$ and the potential matrices $V_\pm(x)$ are given by (3.13) and (4.19) with $\rho = 0$. Parameter ω of the decaying solution $u_0(x)$ is defined in the interval $-1 < \omega < 1$. The six pictures of Figure 1 show the entire spectrum of L, H_+, and H_- for different values of ω (the continuous multimedia animations that show the transformation of eigenvalues when ω decreases are available as 62978_01.avi and 62978_02.avi).

When ω is close to 1 (the gap soliton is close to a small-amplitude sech-soliton), there exists a single nonzero eigenvalue for H_+ and H_- and a single pair of purely imaginary eigenvalues of L (see subplot (1) on Figure 1). The first set of arrays on the subplot (1) indicates that the pair of eigenvalues of L becomes visible at the same value of ω as the eigenvalue of H_+. This correlation between eigenvalues of L and H_+ can be traced throughout the entire parameter domain on the subplots (1)–(6).

When ω decreases, the operator H_- acquires another nonzero eigenvalue by means of the edge bifurcation [13], with no changes in the number of isolated eigenvalues of L (see subplot (2)). The first complex instability occurs near $\omega \approx -0.18$, when the pair of purely imaginary eigenvalues of L collides with the continuous spectrum and emerges as a quartet of complex eigenvalues, with no changes in the number of isolated eigenvalues for H_+ and H_- (see subplot (3)).

The second complex instability occurs at $\omega \approx -0.54$, when the operator H_- acquires a third nonzero eigenvalue and the linearized operator L acquires another quartet of complex eigenvalues (see subplot (4)). The second set of arrays on the subplots (4)–(6) indicates a correlation between these eigenvalues of L and H_-.

When ω decreases further, the operators H_+ and H_- acquire one more isolated eigenvalue, with no change in the spectrum of L (see subplot (5)). Finally, when ω is close to -1 (the gap soliton is close to the large-amplitude algebraic soliton), the third complex instability occurs, correlated with another edge bifurcation in the operator H_- (see subplot (6)). The

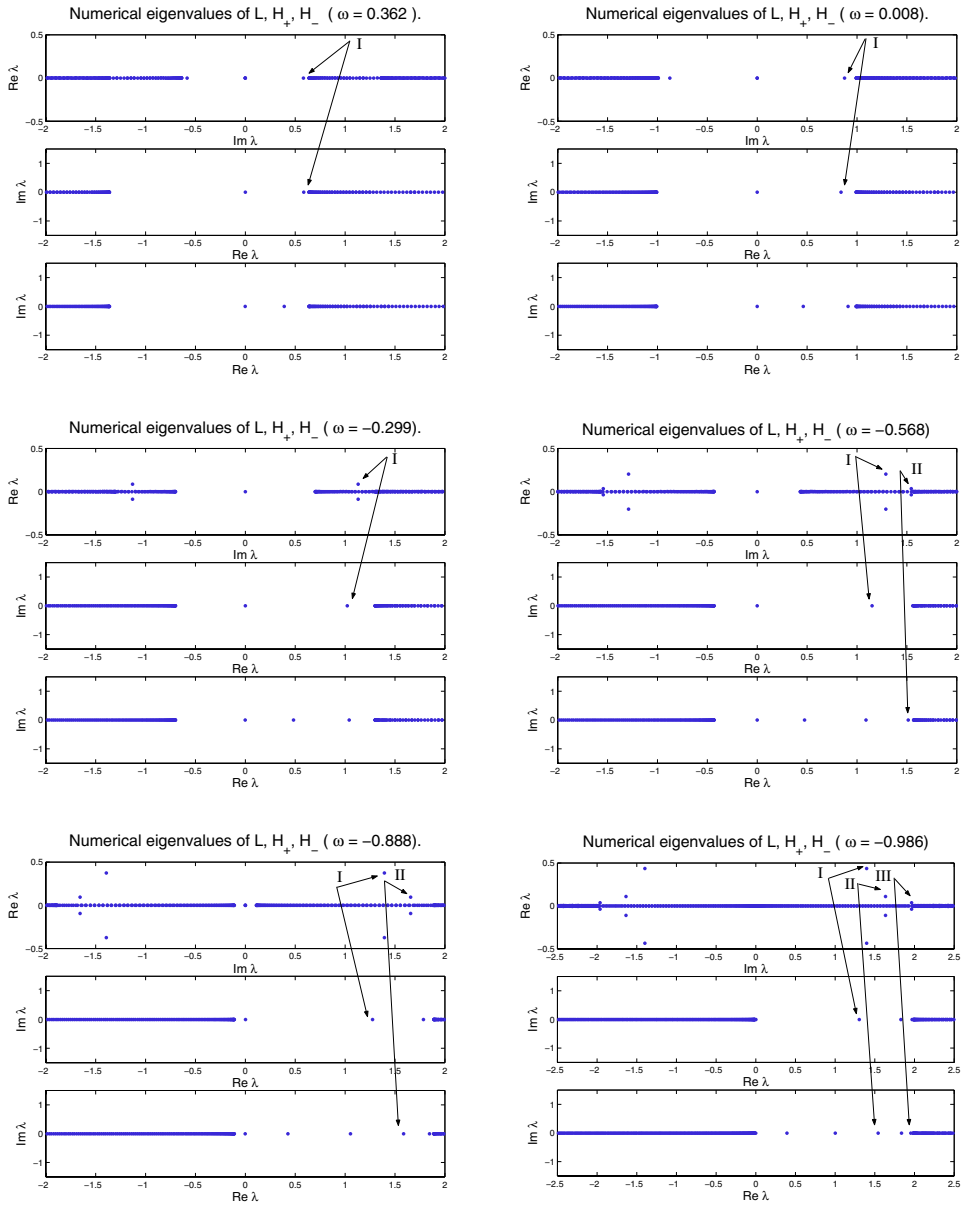

Figure 1. *Eigenvalues and instability bifurcations for the symmetric quartic potential* (2.4) *with* $a_1 = 1$ *and* $a_2 = a_3 = a_4 = 0$. *See also the accompanying animations* (62978_01.avi [724KB] *and* 62978_02.avi [275KB]).

third set of arrays on subplot (6) indicates this correlation. The third complex instability was not detected in the previous numerical studies of the same coupled-mode system [7, 15] (since the previous works did not consider eigenvalues of gap solitons near the limit $\omega = -1$). In a narrow domain near $\omega = -1$, the operator H_+ has two nonzero eigenvalues, the operator H_- has five nonzero eigenvalues, and the operator L has three quartets of complex eigenvalues.

Figure 2 displays the pattern of eigenvalues and instability bifurcations for the symmetric

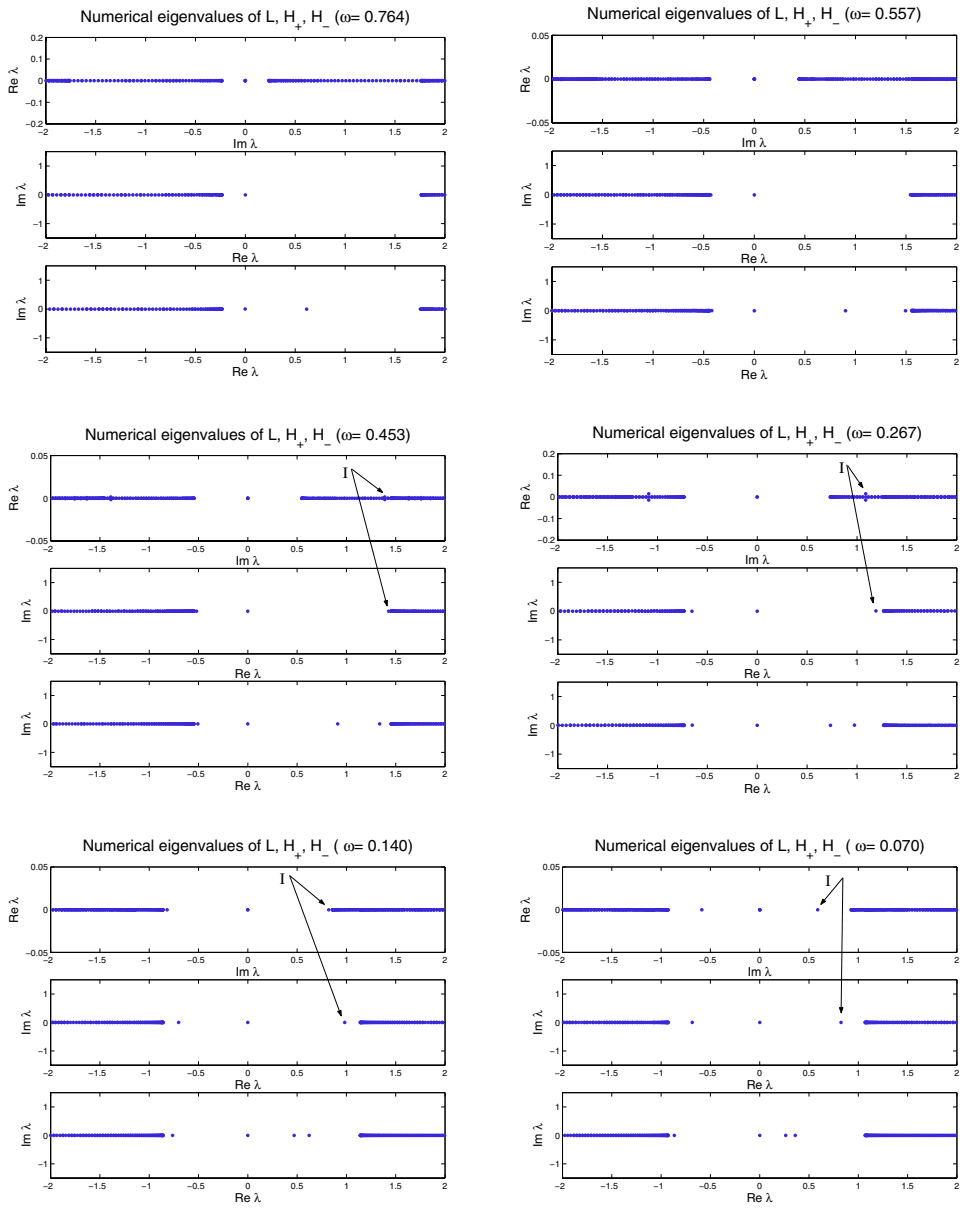

Figure 2. *Eigenvalues and instability bifurcations for the symmetric quartic potential* (2.4) *with* $a_3 = 1$ *and* $a_1 = a_2 = a_4 = 0$.

quartic potential (2.4) with $a_1 = a_2 = a_4 = 0$ and $a_3 = 1$. The decaying solution $u_0(x)$ and the potential matrices $V_\pm(x)$ are given by (3.14) and (4.20) with $0 < \omega < 1$ and $s = 0$. Eigenvalues in the other case $-1 < \omega < 0$ can be found from those in the case $0 < \omega < 1$ by reflections.

When ω is close to 1 (the gap soliton is close to a small-amplitude sech-soliton), there exist one nonzero eigenvalue of H_- and no nonzero eigenvalues of L and H_+ (see subplot

(1)). When ω decreases, two more nonzero eigenvalues bifurcate in H_- from the left and right branches of the continuous spectrum, with no change in the nonzero eigenvalues of L (see subplot (2)). The first complex bifurcation occurs at $\omega \approx 0.45$, when a quartet of complex eigenvalues occurs in L, in correlation with two symmetric edge bifurcations of H_+ from the left and right branches of the continuous spectrum (see subplots (3) and (4)). The first and only set of arrays on the subplots (3)–(6) indicates a correlation between eigenvalues of L and H_+, which is traced through the domain of ω. The inverse complex bifurcation occurs at $\omega \approx 0.15$, when the quartet of complex eigenvalues merges at the edge of the continuous spectrum into a pair of purely imaginary eigenvalues (see subplot (5)). No new eigenvalues emerge for smaller values of ω. When ω is close to 0 (the gap soliton is close to the nondecaying bounded solution), the operator H_+ has two nonzero eigenvalues, the operator H_- has three nonzero eigenvalues, and the operator L has one pair of purely imaginary eigenvalues (see subplot (6)).

We add remarks on two other limiting cases of the symmetric quartic potential (2.4). When $a_1 = a_3 = a_4 = 0$ and $a_2 = 1$, the coupled-mode system is an integrable model and no nonzero eigenvalues of L exist, according to the exact solution of the linearization problem [9]. When $a_1 = a_2 = a_3 = 0$ and $a_4 = \pm 1$, one branch of decaying solutions $u_0(x)$ exists for either sign, according to (3.14) and (3.15). The pattern of eigenvalues and instability bifurcations repeats those in Figure 2.

Our numerical results imply that there exists a correlation between edge bifurcations in the operator L and those in the Dirac operators H_+ and H_-. Analysis of such correlations is beyond the scope of the present paper.

Appendix. Conditions for existence of gap solitons in the homogeneous potential function.

We shall consider the homogeneous potential function $W \in \mathbb{R}$ of the monomial order $2n$ that satisfies conditions 1–3. The general representation of $W(u, \bar{u}, v, \bar{v})$ is given by

$$W = \sum_{s=0}^{n} \sum_{k=0}^{n-s} a_{k,s} \left(u^s \bar{v}^s + \bar{u}^s v^s \right) |u|^{2n-2k-2s} |v|^{2k}, \tag{A.1}$$

where $a_{k,s}$ are real-valued coefficients such that $a_{k_1,s} = a_{k_2,s}$ if $k_1 + k_2 = n - s$ for $s = 0, 1, \ldots, n-1$. Let us introduce new parameters

$$A_s = \sum_{k=0}^{n-s} a_{k,s}, \qquad s = 0, 1, \ldots, n.$$

Using the variables (Q, Θ) defined in (3.4) with $\Phi(x) = \Phi_0 \equiv 0$, we rewrite the ODE system (3.10) in the explicit form

$$\begin{cases} Q' = 2Q \sin(2\Theta) - 2Q^n \sum_{s=0}^{n} s A_s \sin(2s\Theta), \\ \Theta' = -\omega + \cos(2\Theta) - nQ^{n-1} \sum_{s=0}^{n} A_s \cos(2s\Theta). \end{cases} \tag{A.2}$$

There exists a first integral of the system (A.2),

$$-\omega Q + \cos(2\Theta) Q - Q^n \sum_{s=0}^{n} A_s \cos(2s\Theta) = C_0,$$

where $C_0 = 0$ from the zero boundary conditions $Q(x) \to 0$ as $|x| \to \infty$. As a result, the second-order system (A.2) is reduced to the first-order ODE

$$\Theta'(x) = (n-1)(\omega - \cos(2\Theta)), \tag{A.3}$$

while the function $Q(x) \geq 0$ can be found from $\Theta(x)$ as follows:

$$Q^{n-1} = \frac{(\cos(2\Theta) - \omega)}{\sum_{s=0}^{n} A_s \cos(2s\Theta)}. \tag{A.4}$$

We consider the quartic potential function W given by (2.4). Using (A.3) for the case $n = 2$ we obtain

$$\Theta'(x) = \omega - \cos(2\Theta) \tag{A.5}$$

and the correspondence

$$A_0 = \frac{a_1 + a_2 + a_4}{2}, \quad A_1 = 2a_3, \quad A_2 = \frac{a_4}{2}.$$

We rewrite the representation (A.4) for $Q(x)$ as

$$Q = \frac{(t-\omega)}{\phi(t)}, \qquad Q \geq 0, \tag{A.6}$$

where

$$t = \cos(2\Theta), \qquad \phi(t) = a_4 t^2 + 2a_3 t + \frac{a_1 + a_2}{2},$$

such that $t \in [-1, 1]$. Let us consider two cases:

$$\begin{cases} t \geq \omega; & \phi(t) \geq 0 \quad \Rightarrow Q^+, \\ t \leq \omega; & \phi(t) \leq 0 \quad \Rightarrow Q^-. \end{cases} \tag{A.7}$$

We can solve the first-order ODE (A.5) using the substitution $z = \tan(\Theta)$, such that

$$t = \frac{1 - z^2}{1 + z^2}, \qquad z^2 = \frac{1 - t}{1 + t}.$$

After integration with the symmetry constraint $\Theta(0) = 0$, we obtain the solution

$$\left| \frac{(z - \sqrt{\mu})}{(z + \sqrt{\mu})} \right| = e^{2\beta x}, \tag{A.8}$$

where

$$\beta = \sqrt{1 - \omega^2}, \qquad \mu = \frac{1 - \omega}{1 + \omega},$$

and $-1 < \omega < 1$. Two separate cases are considered:

$$|z| \leq \sqrt{\mu}: \quad z = -\sqrt{\mu}\frac{\sinh(\beta x)}{\cosh(\beta x)}, \quad t = \frac{\cosh^2(\beta x) - \mu \sinh^2(\beta x)}{\cosh^2(\beta x) + \mu \sinh^2(\beta x)}, \tag{A.9}$$

where $t \geq \omega$, and

$$|z| \geq \sqrt{\mu}: \quad z = -\sqrt{\mu}\frac{\cosh(\beta x)}{\sinh(\beta x)}, \quad t = \frac{\sinh^2(\beta x) - \mu\cosh^2(\beta x)}{\sinh^2(\beta x) + \mu\cosh^2(\beta x)}, \tag{A.10}$$

where $t \leq \omega$. Let us introduce new parameters

$$\begin{aligned} A &= -2a_3 + a_4 + \frac{a_1 + a_2}{2}, \\ B &= -2a_4 + a_1 + a_2, \\ C &= 2a_3 + a_4 + \frac{a_1 + a_2}{2}. \end{aligned}$$

It is clear that $A = \phi(-1)$ and $C = \phi(1)$. If $t \geq \omega$ and $\phi(t) \geq 0$, it follows from (A.7) and (A.9) that

$$Q^+(x) = \frac{(1-\omega)((\mu+1)\cosh^2(\beta x) - \mu)}{(A\mu^2 + B\mu + C)\cosh^4(\beta x) - (B\mu + 2A\mu^2)\cosh^2(\beta x) + A\mu^2}. \tag{A.11}$$

If $t \leq \omega$ and $\phi(t) \leq 0$, it follows from (A.7) and (A.10) that

$$Q^-(x) = \frac{(\omega-1)((\mu+1)\cosh^2(\beta x) - 1)}{(A\mu^2 + B\mu + C)\cosh^4(\beta x) - (B\mu + 2C)\cosh^2(\beta x) + C}. \tag{A.12}$$

The asymptotic behavior of the function $Q(x)$ at infinity depends on the location of the zeros of the function $\psi(\mu) = A\mu^2 + B\mu + C$. The function $\psi(\mu)$ is related to the function $\phi(t)$; e.g., if $\psi(\mu) = 0$ then $\phi(\omega) = 0$.

A.1. Case $A < 0$, $C > 0$. The quadratic polynomial $\phi(t)$ has exactly one root $\phi(t_1) = 0$ such that $t_1 \in (-1, 1)$. Two branches of decaying solutions with the positive amplitude $Q(x)$ exist. One branch occurs for $t_1 < \omega \leq 1$ with $Q(x) = Q^+(x)$ and the other one occurs for $-1 \leq \omega < t_1$ with $Q(x) = Q^-(x)$. At the point $\omega = t_1$, the solution is bounded and decaying.

A.2. Case $A > 0$, $C > 0$. The quadratic polynomial $\phi(t)$ has no roots or has exactly two roots on $(-1, 1)$. If $\phi(t)$ does not have any roots on $(-1, 1)$, a decaying solution with the positive amplitude $Q(x)$ exists for any $-1 < \omega < 1$ with $Q(x) = Q^+(x)$. If $\phi(t)$ has two roots $\phi(t_1) = 0$ and $\phi(t_2) = 0$ such that $t_1, t_2 \in (-1, 1)$, a decaying solution with $Q(x) = Q^+(x)$ exists only on the interval $\max(t_1, t_2) < \omega \leq 1$. At the point $\omega = \max(t_1, t_2)$, the solution becomes bounded but nondecaying if $t_1 \neq t_2$ and unbounded if $t_1 = t_2$.

A.3. Case $A < 0$, $C < 0$. The quadratic polynomial $\phi(t)$ has no roots or has exactly two roots on $(-1, 1)$. If $\phi(t)$ does not have any roots on $(-1, 1)$, a decaying solution with the positive amplitude $Q(x)$ exists for any $-1 < \omega < 1$ with $Q(x) = Q^-(x)$. If $\phi(t)$ has two roots $\phi(t_1) = 0$ and $\phi(t_2) = 0$ such that $t_1, t_2 \in (-1, 1)$, a decaying solution with $Q(x) = Q^-(x)$ exists only on the interval $-1 \leq \omega < \min(t_1, t_2)$. At the point $\omega = \min(t_1, t_2)$, the solution becomes bounded but nondecaying if $t_1 \neq t_2$ and unbounded if $t_1 = t_2$.

A.4. Case $A > 0$, $C < 0$. No decaying solutions with positive amplitude $Q(x)$ exist.

A.5. Special cases. Two special cases occur when $\phi(1) = 0$ or $\phi(-1) = 0$. If $\phi(1) = 0$, then $Q^+(x)$ has a singularity at $x = 0$ for any $-1 < \omega < 1$. If $\phi(-1) = 0$, then $Q^-(x)$ has a singularity at $x = 0$ for any $-1 < \omega < 1$.

REFERENCES

[1] C. M. de Sterke and J. E. Sipe, *Gap solitons*, Progress in Optics, 33 (1994), pp. 203–260.

[2] Yu. S. Kivshar and G. P. Agrawal, *Optical Solitons: From Fibers to Photonic Crystals*, Academic Press, San Diego, 2003.

[3] L. Pitaevskii and S. Stringari, *Bose-Einstein Condensation*, International Series of Monographs on Physics 116, The Clarendon Press, Oxford University Press, Oxford, UK, 2003.

[4] C. M. de Sterke, D. G. Salinas, and J. E. Sipe, *Coupled-mode theory for light propagation through deep nonlinear gratings*, Phys. Rev. E, 54 (1996), pp. 1969–1989.

[5] D. Agueev and D. Pelinovsky, *Modeling of wave resonances in low-contrast photonic crystals*, SIAM J. Appl. Math., 65 (2005), pp. 1101–1129.

[6] D. E. Pelinovsky, A. A. Sukhorukov, and Yu. S. Kivshar, *Bifurcations and stability of gap solitons in periodic potentials*, Phys. Rev. E, 70 (2004), 036618.

[7] I. V. Barashenkov, D. E. Pelinovsky, and E. V. Zemlyanaya, *Vibrations and oscillatory instabilities of gap solitons*, Phys. Rev. Lett., 80 (1998), pp. 5117–5120.

[8] I. V. Barashenkov and E. V. Zemlyanaya, *Oscillatory instabilities of gap solitons: A numerical study*, Comput. Phys. Comm., 126 (2000), pp. 22–27.

[9] D. J. Kaup and T. I. Lakoba, *The squared eigenfunctions of the massive Thirring model in laboratory coordinates*, J. Math. Phys., 37 (1996), pp. 308–323.

[10] D. J. Kaup and T. I. Lakoba, *Variational method: How it can generate false instabilities*, J. Math. Phys., 37 (1996), pp. 3442–3462.

[11] J. Schollmann, *On the stability of gap solitons*, Phys. A, 288 (2000), pp. 218–224.

[12] J. Schollmann and A. P. Mayer, *Stability analysis for extended models of gap solitary waves*, Phys. Rev. E, 61 (2000), pp. 5830–5838.

[13] T. Kapitula and B. Sandstede, *Edge bifurcations for near integrable systems via Evans function techniques*, SIAM J. Math. Anal., 33 (2002), pp. 1117–1143.

[14] D. E. Pelinovsky and A. Scheel, *Spectral analysis of stationary light transmission in nonlinear photonic structures*, J. Nonlinear Sci., 13 (2003), pp. 347–396.

[15] G. Derks and G. A. Gottwald, *A robust numerical method to study oscillatory instability of gap solitary waves*, SIAM J. Appl. Dyn. Syst., 4 (2005), pp. 140–158.

[16] D. J. B. Lloyd and A. R. Champneys, *Efficient numerical continuation and stability analysis of spatiotemporal quadratic optical solitons*, SIAM J. Sci. Comput., 27 (2005), pp. 759–773.

[17] G. Iooss and M. Adelmeyer, *Topics in Bifurcation Theory and Applications*, 2nd ed., Advanced Ser. Nonlinear Dynam. 3, World Scientific Publishing, River Edge, NJ, 1998.

[18] M. Golubitsky, I. Stewart, and D. G. Schaeffer, *Singularities and Groups in Bifurcation Theory, Vol.* 2, Appl. Math. Sci. 69, Springer-Verlag, New York, 1988.

[19] D. J. Kaup and A. C. Newell, *On the Coleman correspondence and the solution of the massive Thirring model*, Lett. Nuovo Cimento, 20 (1977), pp. 325–331.

[20] D. E. Pelinovsky, *Inertia law for spectral stability of solitary waves in coupled nonlinear Schrodinger equations*, Proc. Roy. Soc. London Ser. A, 461 (2005), pp. 783–812.

[21] Y. Saad, *Numerical Methods for Large Eigenvalue Problems*, Manchester University Press, Manchester, UK, 1992, pp. 60–101.

[22] G. H. Golub and H. A. Van der Vorst, *Eigenvalue computation in the* 20*th century*, J. Comput. Appl. Math., 123 (2000), pp. 35–65.

[23] Y. Saad, *Chebyshev acceleration techniques for solving nonsymmetric eigenvalue problems*, Math. Comp., 42 (1984), pp. 567–588.

[24] L. N. Trefethen, *Spectral Methods in MATLAB*, Software Environ. Tools 10, SIAM, Philadelphia, 2000.